Downloaded from orbit.dtu.dk on: Jun 14, 2021

DTU Library

Integrated analysis of DFIG drive-train and power electronics dynamics during electrical AC faults and wind disturbances

Barahona Garzón, Braulio; Sørensen, Poul Ejnar; Anaya-Lara, Olimpo ; Tande, John

Published in:
Symposium - European Power Electronics and Adjustable Speed Drives Association

Publication date:
2013

Link back to DTU Orbit

Citation (APA):
Barahona Garzón, B., Sørensen, P. E., Anaya-Lara, O., & Tande, J. (2013). Integrated analysis of DFIG drive-train and power electronics dynamics during electrical AC faults and wind disturbances. In *Symposium - European Power Electronics and Adjustable Speed Drives Association* European Power Electronics and Adjustable Speed Drives Association.

General rights
Copyright and moral rights for the publications made accessible in the public portal are retained by the authors and/or other copyright owners and it is a condition of accessing publications that users recognise and abide by the legal requirements associated with these rights.

- Users may download and print one copy of any publication from the public portal for the purpose of private study or research.
- You may not further distribute the material or use it for any profit-making activity or commercial gain
- You may freely distribute the URL identifying the publication in the public portal

If you believe that this document breaches copyright please contact us providing details, and we will remove access to the work immediately and investigate your claim.

Integrated analysis of DFIG drive-train and power electronics dynamics during electrical AC faults and wind disturbances

Braulio Barahona[1,*], Poul Sørensen[1], Olimpo Anaya-Lara[2,3] and John Tande[4]
1) Risø DTU, Roskilde, Denmark. *Email: brab@risoe.dtu.dk
2) Department of Electronic and Electrical Engineering, Institute for Energy and Environment,
University of Strathclyde, Glasgow, UK.
3) Department of Electrical Power Engineering, NTNU, Trondheim, Norway.
4) SINTEF Energy Research, Trondheim, Norway

Acknowledgments

The authors would like to acknowledge NOWITECH for facilitating the collaboration between the institutions involved in the preparation of this research paper. The first author thanks the financial support from Otto Mønsteds Fond, and Risø DTU for his Ph.D. research stay at NTNU.

Keywords

<<integrated dynamic analysis>>, <<DFIG wind turbine>>, <<wind turbine dynamics>>, <<wind disturbances>>, <<grid fault>>, <<HAWC2>> , <<Matlab/Simulink>>

Abstract

The dynamics of a 2 MW DFIG wind turbine are studied during electrical AC faults, and wind disturbances. A simulation platform that couples HAWC2, and Matlab/Simulink was used. High frequencies of the gear box, and power electronics are neglected. It was shown that the dynamics of the dc-link are influenced by turbulence, and wind gusts. An AC fault that triggers protection systems was simulated, and the influence on the dc-link voltage, shaft and tower loading illustrated.

Introduction

The fault ride through (FRT) capabilities of wind turbines are typically assessed disregarding aeroelastic effects, and using relatively simple structural models. Similarly, when considering the impact of wind disturbances on a wind turbine, the impact on electrical components is usually not analyzed. However, such trend is changing as an *integral design* is important to meet power system demands while keeping wind turbines reliable, and economic.

Pursuing an integral design is a multidisciplinary task, in [1] a database of models in different specialized software is created with the vision to use it to optimize designs. However in some cases it may be relevant to analyze the global dynamics of the different subsystems of the wind turbine. Therefore, coupling or combining different specialized software [2, 3, 4, 5, 6], or further developing a given computational code [7, 8, 9] allows an *integrated dynamic analysis* to shed light on the dynamic interactions of different subsystems.

Aeroelastic, and structural models (HAWC2) are coupled with dynamic models of the wind turbine generator, and the power system (Matlab/Simulink). The general objective is to analyze the impact of AC faults and wind disturbances on the structural, and the electrical systems of a DFIG wind turbine. Similar analysis, under an AC fault that does not trip the protection system, can be found in [2] where tower lateral acceleration, and low-speed shaft twist angle are shown to be sensitive. Furthermore, in [5, 10] it is suggested that AC faults impose prohibiting loads on the drive-train gearbox. Detail gearbox, and high-speed shaft models involve a large number of degrees of freedom, while their dominant dynamics are mainly high frequency [5]. The focus of the present work is on dynamics below 50 Hz, and the role of protection system and wind disturbances during a fault.

Simulation tools and models

Wind field, aeroelastic, and mechanical components are simulated in a state-of-the-art software (HAWC2) developed at Risø DTU. The turbulence simulated in the wind field is fully 3D-coherent. Aeroelastic phenomena such as dynamic stall, and the impact of wind shear are included. The mechanical components (i.e. blades, shaft, tower) are each composed of many timoshenko beam elements. Electrical components, control, and power system are simulated in Matlab/Simulink. Technical details of HAWC2-Matlab/Simulink coupling can be found in [11, 6]. The scope is limited to the relevant dynamics in a range up to 50 Hz, disregarding very high frequencies (gearbox dynamics, and converter switching), and the foundation dynamics and loading. Fig. 1 illustrates the interaction of the subsystems modeled.

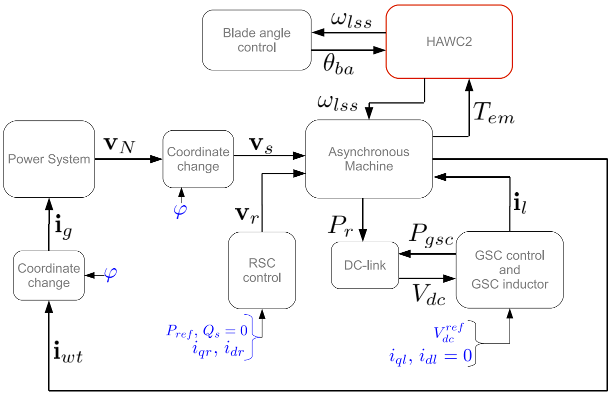

Figure 1: Block diagram illustrating the subsystems modeled with the main variables they exchange, (blue quantities are references or measurements).

HAWC2 model and blade angle control

HAWC2 is based on a multibody formulation, each body consists of many timoshenko beam elements. The model is a generic 2 MW wind turbine that consists of 5 bodies: 3 blades, low-speed shaft (lss), and tower. The gear box, and high speed shaft are considered ideal. HAWC2 (red block in Fig. 1) outputs the speed at the low-speed shaft ω_{lss} to Matlab/Simulink (the rest of the blocks), and reads the blade angle θ_{ba}, and electromagnetic torque T_{em}.

The blade angle control (Fig. 2) is a deterministic adaptive control, that consists of a PI regulator with a scheduled gain [12]. The servo motor that moves the blades to set the blade angle is represented as a first order system.

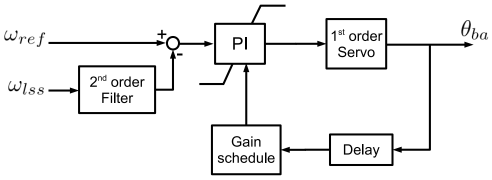

Figure 2: Blade angle control.

Power system

The power system is a double circuit transmission line supplied by an infinite bus $\mathbf{v}_g$. It was modeled as a (lumped-parameter) symmetrical RL-branch in dq-frame. The corresponding voltage equations are those of a 3-phase RL stationary-circuit in an arbitrary reference frame [13]. The reference frame choosen is a synchronously rotating reference frame aligned to $\mathbf{v}_g$ (i.e. system reference frame). Once the elements of the power system are referred to a given voltage level, the voltage equations in matrix form are given by Eq. 1. As can be interpreted from Fig. 1, Eq. 1 is solved for the voltage at the stator terminal in the system reference frame ($\mathbf{v}_N$). This voltage is then changed to the stator voltage $\mathbf{v}_s$, that is on a reference frame oriented with the generator stator flux (SFRF).

$$\mathbf{v}_g - \mathbf{v}_N = \mathbf{R}_g\mathbf{i}_g + \mathbf{L}_g\boldsymbol{\omega}_g + \mathbf{L}_g\dot{\mathbf{i}}_g \tag{1}$$

DFIG generator

The doubly-fed asynchronous generator (DFIG) consists of an asynchronous machine, dc-link, smoothing inductor, rotor-side (RSC) and grid-side converter (GSC) with their corresponding controls. The well known full-order dynamic model of asynchronous machine was implemented with flux linkages as state variables [13], in matrix form it can be expressed by Eq. 2.

$$\begin{bmatrix}\dot{\boldsymbol{\lambda}}_{dqs}\\ \dot{\boldsymbol{\lambda}}_{dqr}\end{bmatrix} = \boldsymbol{\mathcal{M}}\begin{bmatrix}\boldsymbol{\lambda}_{dqs}\\ \boldsymbol{\lambda}_{dqr}\end{bmatrix} + \begin{bmatrix}\mathbf{v}_{dqs}\\ \mathbf{v}_{dqr}\end{bmatrix} \tag{2}$$

The dynamics of the dc-link neglecting power losses [14, 15] are represented according to Eq. 3. The active power P_{gsc}, flowing through the smoothing inductor X_{sl}, is calculated according to Eq. 4 based on the concept of power transfered between two sources [16].

$$V_{dc} = \sqrt{\frac{2}{C_{dc}}\int (P_r - P_{gsc})dt} \tag{3}$$

$$P_{gsc} = \frac{3}{2}\frac{|\mathbf{v}_{gsc}||\mathbf{v}_{dqs}|}{X_{sl}}\sin\delta \tag{4}$$

RSC and GSC are considered considered controllable sources, their control is implemented as generic cascade proportional-integral (PI) controls [14, 12, 17]. Fig. 3 shows these control loops, RSC controls total active power P_t, and stator reactive power Q_s. GSC controls the dc-link voltage V_{dc}, and operate the converter at unity power factor (i.e. $i_{dl}^{ref} = 0$).

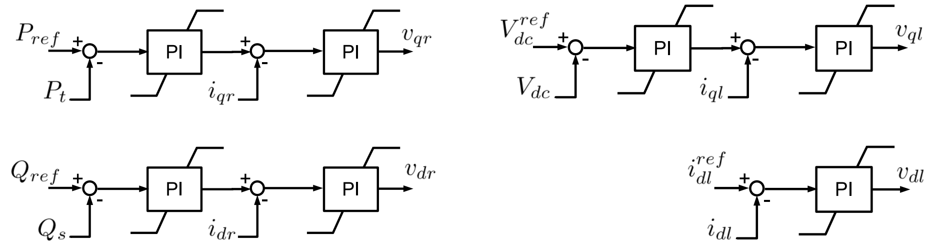

(a) Rotor side converter.

(b) Grid side converter

Figure 3: Generator control.

A passive (or so called single shot) crowbar is used to protect the RSC from over currents [15]. It consists of a switch that short-circuits the rotor through an external resistance, thereby isolating the RSC. It has a duty cycle of 0.5 s, it triggers when $|\mathbf{i}_r| \geq 2$ p.u., and it removes if $|\mathbf{v}_s| \approx 1$ p.u., and if the duty cycle is met. For the reconnection of the RSC once the crowbar is removed, the RSC control is reset to avoid larger transients [14].

Simulation results

The cases simulated aim at analyzing the dynamics of the various subsystems of a DFIG wind turbine during an AC fault, and wind disturbances while operating at full load under nominal wind speed. First the intention is on one hand study the wind turbine structural dynamics, particularly in the drive-train (i.e. low-speed shaft) during the AC fault, while also considering the influence of wind gusts and turbulence in the dynamics of the power electronics (i.e. DC-link voltage). In the second case the role of over-current protection system of DFIG on the wind turbine structural dynamics during an AC fault is the focus.

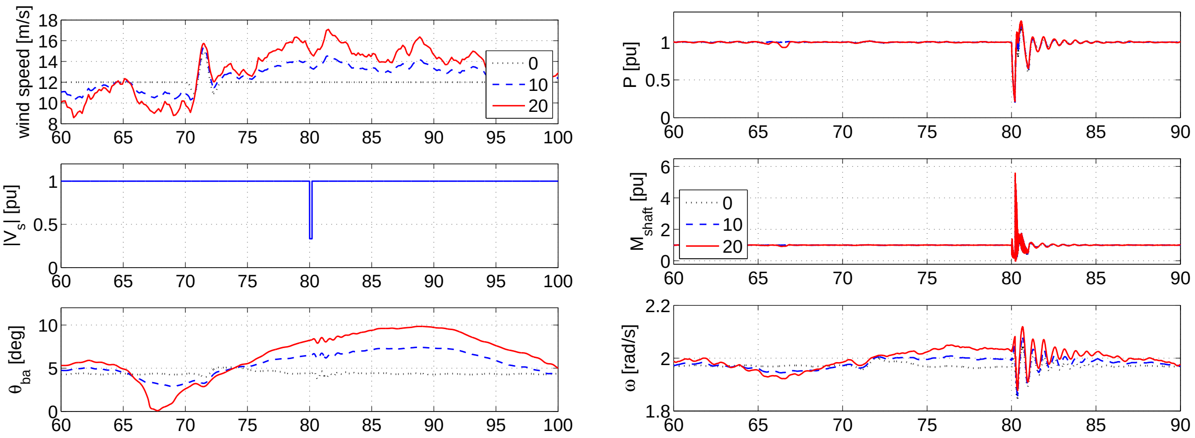

(a) Wind speed, stator voltage, and blade angle.

(b) Electrical power, moment at lss, and speed at lss.

Figure 4: Case 1. Response to wind gust, turbulent wind, and AC fault.

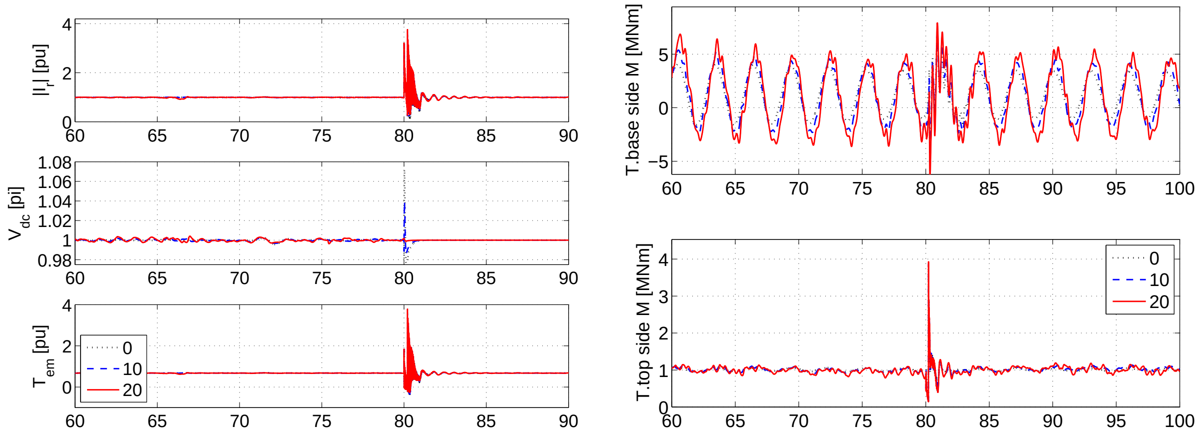

(c) Rotor current, DC voltage, and electromagnetic torque.

(d) Tower base, and tower top side-to-side moments.

Figure 4: Case 1. Response to wind gust, turbulent wind, and AC fault.

Wind disturbances and fault

The first simulation case Fig. 4 consists of simulations with 0%, 10%, and 20% turbulence. A 3 m/s wind gust is simulated at $t = 70$ s. The wind gust provoques variations of the speed ω in Fig. 4b (i.e. speed at low-speed shaft). These variations induce fluctuations in the power that are reflected in the DC-link voltage (Fig. 4c), however not dramatically.

A symmetrical AC fault at one of the lines of the double circuit is simulated at $t = 80$ s, the voltage drops to about 0.2 p.u., the fault is cleared after 200 ms (Fig. 4a). The crowbar external resistance is disabled, and the RSC is simply disconnected once the fault occurs. From Fig. 4b it can be seen that as ω is generally fluctuating more with higher turbulence, also during the fault the fluctuations of ω are larger with higher turbulence. Evidently, the same behavior is expected from other structural and electrical variables. This can be observed from Fig. 4d in the tower side-to-side moments. However, in the electrical variables the influence of the turbulence is not so noticeable, for example in the rotor current, DC-link voltage and electromagnetic torque shown in Fig. 4c.

AC fault with over-current protection

In the second simulation case Fig. 5, a symmetrical AC fault in one of the lines of the double circuit is simulated at $t = 60$ s with the same characteristics as in the previous case, while the wind is kept

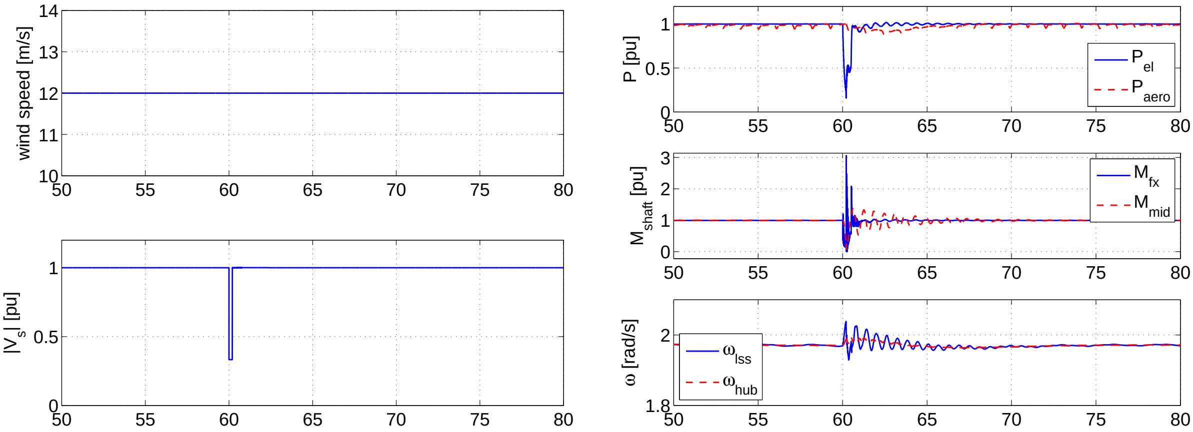

(a) Wind speed, and stator voltage. (b) Power, shaft moments, and speed at hub and at lss

Figure 5: Case 2. Response to AC fault with over-current protection

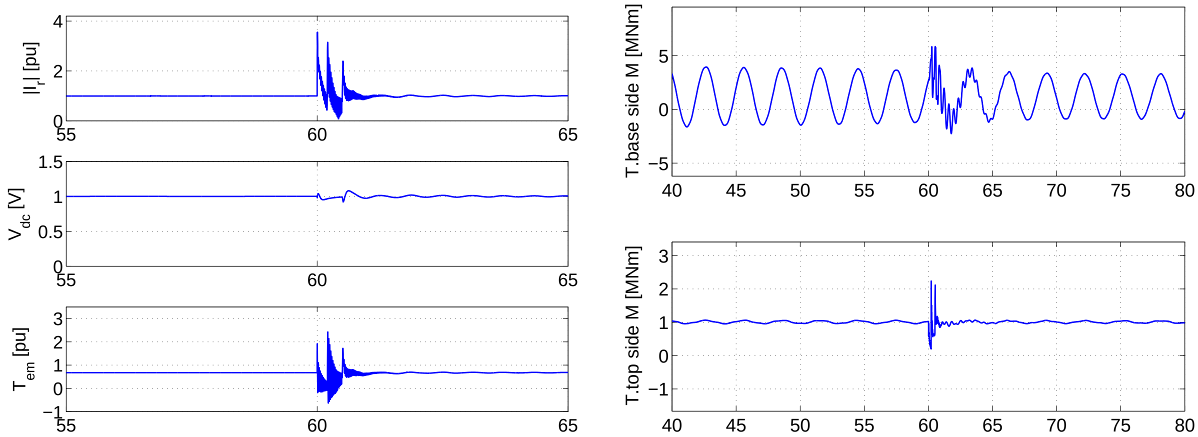

(c) Rotor current magnitude, DC voltage, and electromagnetic torque (d) Tower base, and tower top side-to-side moments

Figure 5: Case 2. Response to AC fault with over-current protection

constant. The over-current protection (i.e. passive crowbar) for the RSC triggers itself immediately after the fault, and removes once the voltage is reestablished. Fig. 5b shows on the top plot the electrical, and the aerodynamic power, the electrical power falls abruptly during the fault, while the aerodynamic power fluctuates after the fault due to the changes of electromagnetic torque that impose fluctuating loads on the shaft (M_{fx} and M_{mid} in middle plot) that in turn produce changes of speed ω_{lss}, and ultimately oscillations of the hub speed ω_{hub} (bottom plot).

Fig. 5c, illustrates the effect of the fault, and the role of the over-current protection in the rotor current $|I_r|$, dc-link voltage V_{dc}, and electromagnetic torque T_{em}. Namely, it can be observed how V_{dc} responds after the fault, once the protection is removed. Fig. 5d shows that the loads on tower top side-to-side moment during the fault, and the removal of the protection can reach relatively high maximum values.

Conclusions and further work

The dynamics of structural, and electrical subsystems of a DFIG wind turbine were simulated with HAWC2-Matlab/Simulink. The influence of wind disturbances on the dc-link voltage of the power electronics was illustrated with simulations of turbulent wind, and a wind gust, while the dc-link voltage is sensible such disturbances, the simulations showed that this influence in not dramatic. However, this is very dependent on the dimensions of the system, and the design of the control, therefore a parametric study would yield more general results for this wind turbine topology.

The influence of electrical disturbances was also illustrated. For example, simulations showed the mechanical loads imposed on the low-speed shaft during the fault, it was observed that the removal of the over-current protection may impose relatively large loading on the tower top side-to-side moment. This is however, dependent on how the electromagnetic torque fluctuations transferred through the speed/torque of the generator rotor are propagated through the nacelle and into the tower,the simulations presented here represent a worst case.

References

[1] F. Iov, A. D. Hansen, P. Sørensen, and F. Blaabjerg, "Simulation platform to model, optimize and design wind turbines," Tech. Rep. ISBN 87-89179-45-5, Aalborg University and Risø National Laboratory, 2004.

[2] R. Fadaeinedjad, M. Moallem, and G. Moschopoulos, "Simulation of a wind turbine with doubly fed induction generator by fast and simulink," *IEEE Transactions on Energy Conversion*, vol. 23, pp. 690–700, 2008.

[3] F. M. Huges, O. Anaya-Lara, G. Ramtharan, N. Jenkins, and G. Strbac, "Influence of Tower Shadow and Wind Turbulence on the Performance of Power System Stabilizers for DFIG-Based Wind Farms," *IEEE Transactions on Energy Conversion*, vol. 23, pp. 519–528, 2008.

[4] A. D. Hansen, N. A. Cutululis, H. Markou, and P. Sørensen, "Impact of fault ride-through requirements on fixed-speed wind turbine structural loads," *Wind Energy*, 2010.

[5] J. Sanz-Corretge, A. García-Barace, and I. Egaña, "Load transient analysis of wind turbine drive train under grid disturbances," in *European Wind Energy Conference*, 2010.

[6] B. Barahona, L. C. Henriksen, A. D. Hansen, N. A. Cutululis, and P. Sørensen, "Coupling of HAWC2 and Matlab: Towards an Integrated Simulation Platform," in *European Wind Energy Conference*, April 2010.

[7] A. Heege, Y. Radovcic, and J. Betran, "Fatigue load computation of wind turbine gearboxes by coupled structural, mechanism and aerodynamic analysis," *DEWI Magazin*, vol. 28, pp. 61 – 68, 2006.

[8] G. Ramtharan, N. Jenkins, O. Anaya-Lara, and E. Bossanyi, "Influence of rotor structural dynamics representations on the electrical transient performance of fsig and dfig wind turbines," *Wind Energy*, vol. 10, pp. 293–301, March 2007.

[9] G. Ramtharan, N. Chris, and B. Ervin, "Importance of advanced simulations of electrical transients in wind turbines," in *European Wind Energy Conference*, April 2010.

[10] D. Aguglia and R. Rebeschini, "Power transformer role for gearbox mechanical stress mitigation during voltage dips applied to doubly-fed induction generator based wind turbines," in *European Wind Energy Conference*, 2010.

[11] B. Barahona, P. B. Adersen, A. D. Hansen, N. A. Cutululis, and P. Sørensen, "Integrated design of wind power systems: MATLAB-HAWC2 interface," in *50th International Conference of Scandinavian Simulation Society (SIMS 50)*, 2009.

[12] A. D. Hansen and G. Michalke, "Fault ride-through capability of DFIG wind turbines," *Renewable Energy*, vol. 32, pp. 1594 – 1610, December 2006.

[13] P. C. Krause, O. Wasynczuk, and S. D. Sudhoff, *Analysis of Electric Machinery and Drive Systems*. IEEE Press Series on Power Engineering, WileyBlackwell, 2002.

[14] V. Akhmatov, *Analysis of Dynamic Behaviour of Electric Power Systems with Large Amount of Wind Power*. PhD thesis, Technical University of Denmark, 2003.

[15] O. Anaya-Lara, N. Jenkins, J. Ekanayake, P. Cartwright, and M. Huges, *Wind Energy Generation: Modelling and Control*. Wiley, 2009.

[16] P. Kundur, *Power System Stability and Control*. McGraw-Hill, 1994.

[17] G. Michalke, *Variable Speed Wind Turbines - Modelling, Control and Impact on Power Systems*. PhD thesis, Darmstadt Technical University, 2008.